Journal of Colloid and Interface Science **211,** 39–44 (1999)
Article ID jcis.1998.5986, available online at http://www.idealibrary.com on IDEAL®

Mercury Intrusion Porosimetry and Image Analysis of Cement-Based Materials

A. B. Abell, K. L. Willis, and D. A. Lange[1]

University of Illinois, Department of Civil Engineering, Urbana, Illinois 61821

Received December 19, 1997; accepted November 18, 1998

Mercury intrusion porosimetry (MIP) is a widely used technique for characterizing the distribution of pore sizes in cement-based materials. It is a simple and quick indirect technique, but it has limitations when applied to materials that have irregular pore geometry. The relationship between MIP results and the actual pore distribution and connectivity can be better understood with the use of image analysis. This paper discusses the use of MIP to describe the pore structure of cements and the efforts to validate the technique with microscopy. In particular, a study using molten Wood's metal as an alternate intrusion liquid that is solid in the pores at room temperature and can be examined by scanning electron microscopy will be presented. Results of the image analysis and the intrusion behavior of Portland cement mortars will be discussed.

Key Words: **mercury porosimetry; Wood's metal; image analysis; porosity; cement-based materials.**

INTRODUCTION

A cement-based engineering material, such as mortar or concrete, is a composite of a binding matrix primarily containing hydrated Portland cement and aggregate. The hydrated cement is a highly porous material with a continuous range of pore sizes from nanometers to micrometers. The pores, which are contained within the calcium silicate hydrate phase of the cement paste (C-S-H gel) and are the remnants of space previously occupied by mixing water (referred to as capillary pores) that are partially filled by a variety of hydrated cement products, have irregular geometry. Although the quantity of pores is great in cement-based materials, the permeability of these systems is low as Powers (1) pointed out in his pioneering work. The amount of porosity and connectivity strongly influences the material properties, particularly the strength and permeability, which affect the resistance to harmful penetrants. The degree to which chloride ions can diffuse through the pore water of reinforced concrete and attack the passive film protecting the reinforcing steel from expansive corrosion has a direct impact on the durability of structures such as bridges and parking decks.

[1] To whom correspondence should be addressed.

Because of the complexity of the pore structure of these materials, measuring total porosity and size distribution is difficult. The methods typically used, which are mercury intrusion porosimetry (MIP), water vapor adsorption, and nitrogen adsorption, assume that the geometry of the pores is regular, that the pores are interconnected, and that the size distribution is not affected by the loss of water in the pores upon drying. A single technique is not able to characterize the whole range of pore sizes found in cement materials. MIP can measure larger capillary pores (0.005–10 μm), whereas the adsorption techniques can describe the C-S-H gel porosity ($<$0.03 μm).

Microscopy has also been used extensively to observe the microstructure of cement-based materials. Scanning electron microscopy (SEM) is capable of observing the microstructural scale that includes the capillary porosity. In conjunction with a backscatter electron (BSE) detector, the chemical composition of the microstructure is represented in the images by gray level variation. Pores appear very dark, which allows them to be distinguished and quantified by image analysis of the 2-D sections (2). Information about the 3-D pore network or connectivity cannot be directly observed.

Because MIP does provide information about the connectivity of the pores and microscopy reveals information about pore geometry, researchers are interested in combining the techniques for a more complete picture of pore systems.

MERCURY INTRUSION POROSIMETRY

Mercury intrusion porosimetry is based on the premise that a nonwetting liquid (one having a contact angle greater than 90°) will only intrude capillaries under pressure. The relationship between the pressure and capillary diameter is described by Washburn (3) as

$$P = \frac{-4\gamma \cos \theta}{d},$$

where P = pressure, γ = surface tension of the liquid, θ = contact angle of the liquid, and d = diameter of the capillary. Mercury must be forced using pressure into the pores of a

0021-9797/99 $30.00

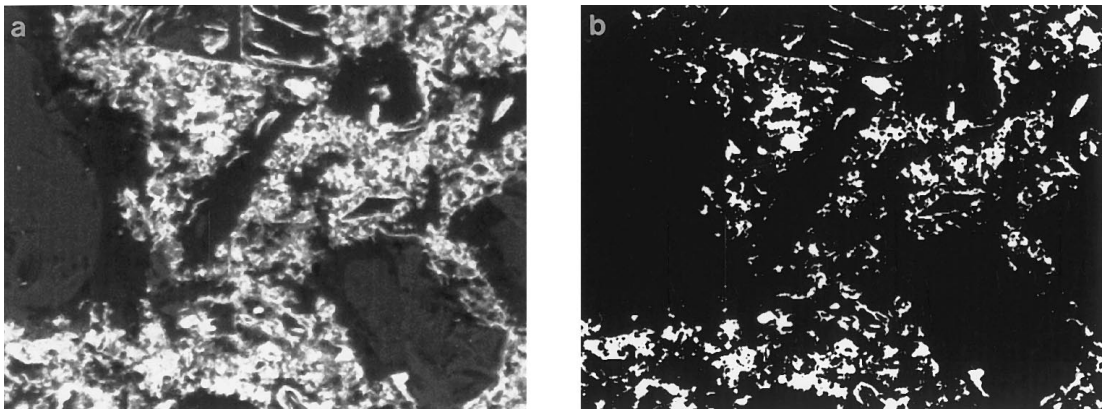

FIG. 1. 0.4 w/c mortar sample intruded at 34.5 MPa (1500×, field width = 85 μm). (a) BSE image, (b) binary image.

material. The pore size distribution is determined from the volume intruded at each pressure increment. Total porosity is determined from the total volume intruded.

The MIP technique is widely used because of its ease and simplicity. However, it does not measure the true distribution of sizes for pore geometries found in cement-based materials. For these systems, large internal pores are accessible by very narrow throats. The MIP technique misrepresents the size of these pores as having the diameter of their throats. This bias is referred to as the "ink bottle" effect.

For cement-based materials the pore size distributions are useful for comparing similar systems and for obtaining a measure of percolation. The continuous pore diameter, which is determined from the largest differential intruded volume with respect to diameter, identifies where percolation has occurred. This diameter has been referred to in other literature as the effective or threshold diameter.

An additional limitation of MIP to the "ink bottle" effect is the influence on the contact angle for mercury with cement-based materials by the preparation of the sample. MIP requires that the sample be dry, which changes the pore structure. A 13° change in contact angle between P-dried and oven-dried cement pastes has been found to reduced the diameter intruded at a given pressure by 30% (4). The contact angle may also change depending upon the roughness of the surface (5). Sample drying has also been implicated in the damage thought to be caused to the cement microstructure under pressure with mercury (6). Lower pressurization over the typical pore size range to reduce the possibility of crushing was attained by intruding mercury that had been modified with a solution of sodium (7).

In order to understand the limitations of MIP for cement-based materials, microscopy and alternative methods of porosimetry have been employed. Lange, *et al.* (8) imaged the pore structure using BSE microscopy, evaluated pore size and shape with respect to mechanical properties, and compared the size distributions to MIP results for pastes and mortars with and without silica fume. They found that image analysis could provide more information about larger pores, that the shapes of the pore size distributions were similar to the curves from MIP, and that the pore sizes were three orders of magnitude larger than the sizes from MIP. Diamond and Leeman (9) also compared MIP to pore size distributions of equivalent diameters determined by image analysis and found the same shift in sizes.

Dullien and Mehta (10) compared size distribution of salt particles by statistical methods. The salt was packed in a bed, infiltrated with molten Wood's metal (a low-melting point alloy), sectioned after the metal had solidified, and photographed. The salt was leached and the porous skeleton was investigated with MIP. The pore size distribution from MIP failed to show the existence of the majority of observed pores because of the small entries to those pores. Dullien and Dhawan (11) later compared pore volume distributions from MIP to those determined by pore size analysis from photomicroscopy of sandstones intruded with Wood's metal and found that the volume contribution from entry pores was significantly smaller than from larger pores behind the entry. Wood's metal intrusion has also been applied to concrete to investigate paste/aggregate interfacial porosity (12). Recently the alternate in-

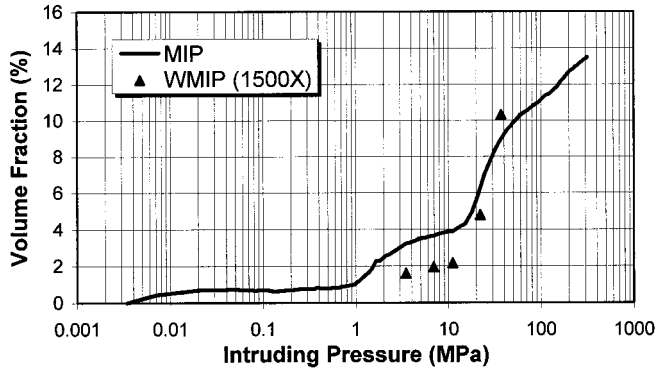

FIG. 2. Volume fraction by image analysis and MIP for the 0.4 w/c mortar.

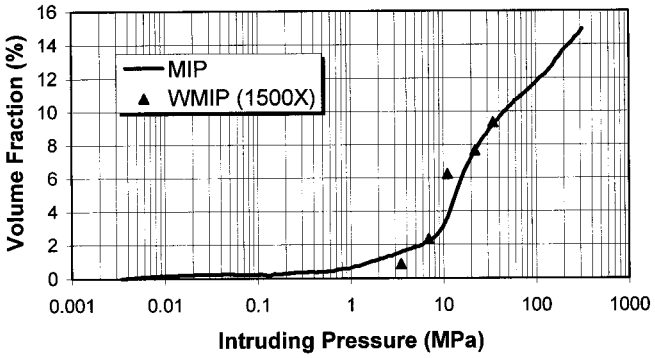

FIG. 3. Volume fraction by image analysis and MIP for the 0.6 w/c mortar.

trusion technique has been applied to Portland cement mortars in conjunction with image analysis of BSE micrographs.

WOOD'S METAL INTRUSION POROSIMETRY

Wood's metal intrusion porosimetry (WMIP) is a technique that replaces the intruding mercury of MIP with an alloy that has a melting point of 65.5°C and is solid at room temperature. Molten Wood's metal is nonwetting and behaves similar to liquid mercury used in mercury porosimetry (11). For this study of mortars the contact angle for Wood's metal was measured from digital photographs of molten drops on a flat mortar surface under ambient conditions. The measured range of 133–140° is the same as widely accepted values for contact angles for mercury. The intrusion procedure includes evacuating a sample and Wood's metal contained within the pressure vessel of an autoclave, heating the autoclave to liquify the metal inserted with the sample, and applying pressure to the vessel with nitrogen gas. The intruded samples can be sectioned and observed with electron microscopy using a backscatter detector. The large mean atomic number of the metal with respect to the mean atomic number of the mortar phases results in a high contrast of the brightness of the metal-filled pores that can be identified by image analysis.

EXPERIMENT TECHNIQUE

Two Portland cement mortars with different water cement ratios were chosen for investigation of the pore structure. The properties of the fresh and hardened mortar were measured, and the hardened samples were intruded with Wood's metal, sectioned, and imaged using a scanning electron microscope.

The materials tested were mortars of ordinary Portland cement (OPC) with water to cement ratios (w/c) of 0.4 and 0.6 with a ratio of 1:2 by weight of cement to ASTM 20/30 silica sand. The air content of the fresh mortars measured by ASTM C185 was 8 and 4% for the 0.4 and 0.6 w/c mixes, respectively. Beams were cast and compacted with vibration and moist-cured for 14 days.

The samples were cored from the beams. Core sections, 1 cm ($\frac{3}{8}$ in.) in diameter and roughly 2 cm long, were oven-dried. A glass test tube containing a sample and solid Wood's metal was placed in the pressure vessel and evacuated to 6.7 Pa (50 μm Hg) to replicate the evacuation in the MIP test. The vessel was heated to 100°C under vacuum, vented, and pressurized. One sample of each mortar was pressurized to 34.5, 20.7, 10.3, 6.9, and 3.4 MPa (5000, 3000, 1500, 1000, and 500 psi) using nitrogen gas. The heat was maintained for approximately 15 min, and then the vessel was allowed to cool to room temperature outside the autoclave while still under pressure.

Each of the 10 samples was prepared for BSE microscopy by sectioning to expose three surfaces. These surfaces were impregnated with epoxy, ground, and polished. Twenty digital images of each cut surface were recorded at a magnification of 1500× with a voltage of 15 keV.

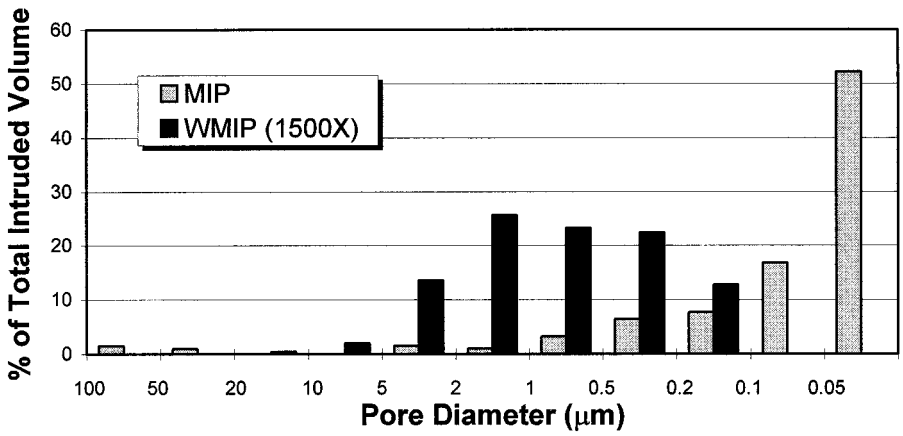

FIG. 4. MIP and Wood's metal pore size distribution for the 0.6 w/c mortar.

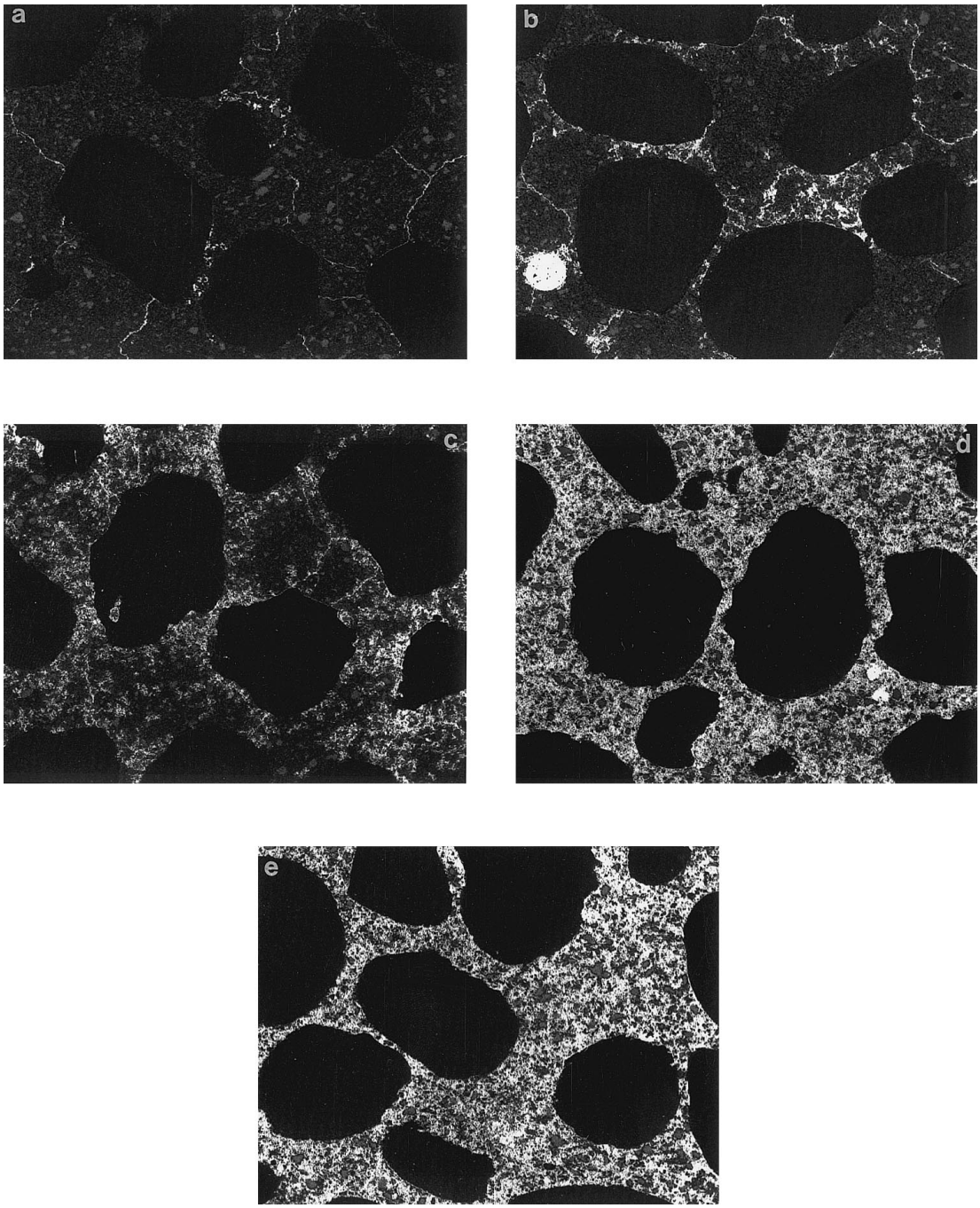

FIG. 5. BSE micrographs of 0.6 w/c pressurized samples (50×, field width = 2.6 mm). (a) 3.4 MPa, (b) 6.9 MPa, (c) 10.3 MPa, (d) 20.7 MPa, (e) 34.5 MPa.

IMAGE ANALYSIS AND POROSITY

The digital micrographs were evaluated on a Macintosh using the public domain NIH Image program and its macro programming language (developed at the U.S. National Institutes of Health and available on the Internet at http://rsb.info.nih.gov/nih-image/). The intruded pores were identified by thresholding the brightness of the pores to produce a binary image. The thresholding process differentiated between the brightest areas of Wood's metal from the intermediate brightnesses that were a result of the interaction of the electron beam in the paste having low mean atomic number and metal having high mean atomic number. Figure 1 illustrates the recorded and binary images. The area fraction of the metal in the binary

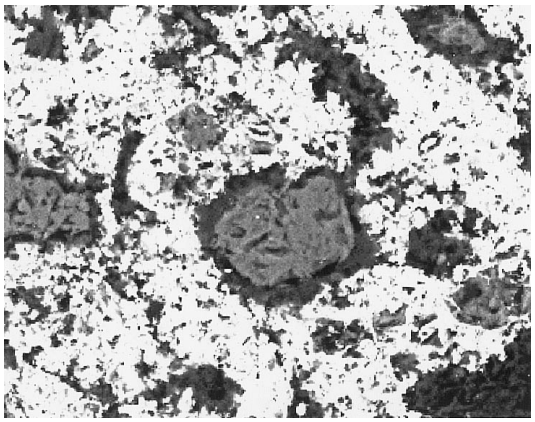

FIG. 6. BSE Micrograph of 0.6 w/c mortar and intrusion of C-S-H (1500×, field width = 60 μm).

image was computed and the particle areas and sizes were analyzed. Each pixel of the digital image was measured at 0.081×0.081 μm. The volume fraction of the intruded metal which can be related directly to the area fraction (13) was determined using the average of the area fractions calculated from the images for each sample.

Figure 2 and Figure 3 present the results from the image analysis and MIP. There is good agreement between the volume fraction of mercury intruded and the volume fraction of Wood's metal intruded as determined by image analysis. The mercury volume fraction reported by MIP and the Wood's metal volume fraction reported by image analysis are comparable parameters that show good agreement in this study. The image analysis and MIP results indicate a threshold (constricting) diameter for both mortars at a pressure of 10 MPa.

The pore size distributions for the pressure range up to 34.5 MPa for MIP and WMIP are compared in Fig. 4. Figure 4 is a histogram that indicates the amount of porosity with each bin. For the WMIP analysis the amount of porosity for a given bin is determined by computing the sum of the areas of individual pores within the bin size range and dividing by the total intruded volume of Wood's metal. For example, 26% of the pores in the WMIP analysis were between 1 and 2 μm average pore diameter. For the MIP analysis the amount of porosity for each bin is determined directly from the intrusion curve in Fig. 3, and the volume of porosity within each bin size range is divided by the total intruded mercury. The intent of Fig. 4 is to illustrate how MIP and image analysis differ in their assignment of pore sizes. The image analysis showed a greater quantity of larger pores than MIP. MIP indicated that most pores are under 0.005 μm in diameter. But microscopic investigation reveals most pores are between 0.02 and 50 μm in average diameter. The results confirm the problem created by the "ink bottle" effect that inflates the volume of smaller pores due to the presence of larger pores behind the bottlenecks.

The intrusion process can also be observed from the micrographs of samples intruded at increasing pressures. Figure 5 shows a series of images for 0.6 w/c mortar samples. At 3.4 MPa (Fig. 5a) the metal has infiltrated through cracks and into large voids. Unconnected large voids remain empty. At 6.9 MPa (Fig. 5b) the metal intruding the cracks continues to fill large connected voids, and the very porous regions between closely spaced aggregate particles (shown as solid black) are filled. In Fig. 5c, the intrusion at 10.3 MPa has noticeably increased and is evident by a saturation of the interfacial regions surrounding the aggregate particles and infiltration into some of the groundmass (bulk cement paste). This pressure is near the second threshold diameter measured by MIP and microscopy indicates that the constriction is in the groundmass. In Fig. 5d, the sample was pressurized to 20.7 MPa resulting in a relatively uniform intrusion of the groundmass. At 34.5 MPa (Fig. 5e) the concentration of the intrusion into the groundmass has increased. At this pressure, the pore diameters measured by MIP are 0.036 μm, which is within the range of the gel pore sizes. The increased concentration of Wood's metal in the groundmass corresponds to the filling of the gel porosity.

Further observation of the intrusion of the groundmass reveals some information about the nature of the C-S-H gel. Figure 6 shows that while the groundmass has been fully saturated at 34.5 MPa, the area surrounding unhydrated cement grains has not. The groundmass, which is composed of C-S-H gel formed at the early stages of hydration, is much more porous than the dense C-S-H formed at the later stages. Further investigation using higher pressure for the Wood's metal porosimetry is needed to further quantify these differences.

SUMMARY

The Wood's metal intrusion technique and image analysis were applied to cement-based materials for a better understanding of the pore structure and its relationship to the pore structure measured by MIP. The findings show that the limitation of MIP due to the assumption of regular pore geometry can be confirmed by substitution of the intruding liquid with one that remains solid in the pores of mortar samples after pressurization and by quantitative measurement of the infiltrated system. The volume intruded by WMIP agrees well with MIP and the distribution in pore sizes from WMIP indicates that more large pores are present. The micrographs also enabled the intrusion process to be interpreted and indicate that there is a difference in porosity between the early and late C-S-H hydration products.

ACKNOWLEDGMENTS

This research was supported by the NSF Center for Advanced Cement-Based Materials (NSF Grant DMR 88808432-01), and NSF Career Award (NSF Grant CMS 96-23467).

REFERENCES

1. Powers, T. C., Portland Cement Association R&D Bulletin 90, 1958.
2. Scrivener, K. L., *Mater. Res. Soc. Symp. Proc.* **137,** 129 (1989).

3. Washburn, E. W., *in* "Proceedings of the National Academy of Sciences," Vol. 7, p. 115. Proc. Natl. Acad. Sci., 1921.
4. Winslow, D. N., and Diamond, S., *JOM* JMLSA **5,** 564 (1970).
5. Eick, J. D., Good, R. J., and Newman, A. W., *J. Colloid Interface Sci.* **53,** 235 (1975).
6. Feldman, R. F., *J. Am. Ceramic Soc.* **67,** 30 (1984).
7. Winslow, D., *Mater. Res. Soc. Symp. Proc.* **137,** 93 (1989).
8. Lange, D. A., Jennings, H. M., and Shah, S. P., *Cem. Concrete Res.* **24,** 841 (1994).
9. Diamond, S., and Leeman, M. E., *Mater. Res. Soc. Symp. Proc.* **370,** 217 (1995).
10. Dullien, F. A. L., and Mehta, P. N., *Powder Technol.* **5,** 179 (1972).
11. Dullien, F. A. L., and Dhawan, G. K., *J. Colloid Interface Sci.* **52,** 129 (1975).
12. crivener, K. L., and Nemati, K. M., *Cem. Concrete Res.* **26,** 35 (1996).
13. Underwood, E. E., "Quantitative Stereology," pp. 1–147. Addison-Wesley, Reading, 1970.